CASE COPY

COLD-AIR PERFORMANCE OF A TIP TURBINE DESIGNED TO DRIVE A LIFT FAN

I - Baseline Performance

Jeffrey E. Haas, Milton G. Kofskey,
Glen M. Hotz, and Samuel M. Futral, Jr.

Lewis Research Center
and U.S. Army Air Mobility R&D Laboratory
Cleveland, Ohio 44135

1. Report No. NASA TM X-3452	2. Government Accession No.	3. Recipient's Catalog No.
4. Title and Subtitle COLD-AIR PERFORMANCE OF A TIP TURBINE DESIGNED TO DRIVE A LIFT FAN I - BASELINE PERFORMANCE		5. Report Date December 1975
		6. Performing Organization Code
7. Author(s) Jeffrey E. Haas, Milton G. Kofskey, Glen M. Hotz, and Samuel M. Futral, Jr.		8. Performing Organization Report No. E-8754
		10. Work Unit No. 505-05
9. Performing Organization Name and Address Lewis Research Center National Aeronautics and Space Administration Cleveland, Ohio 44135		
		11. Contract or Grant No.
		13. Type of Report and Period Covered Technical Memorandum
12. Sponsoring Agency Name and Address National Aeronautics and Space Administration Washington, D.C. 20546		
		14. Sponsoring Agency Code

15. Supplementary Notes

16. Abstract

Full admission baseline performance was obtained for a 0.4 linear scale of the LF460 lift fan turbine over a range of speeds and pressure ratios without leakage air. These cold-air tests covered a range of speeds from 40 to 140 percent of design equivalent speed and a range of scroll inlet to diffuser exit static pressure ratios from 2.0 to 4.2. Results are presented in terms of specific work, torque, mass flow, efficiency, and total pressure drop.

17. Key Words (Suggested by Author(s)) Tip turbine; Lift fan turbine; VTOL aircraft; STOL aircraft; Aerodynamic performance; Efficiency	18. Distribution Statement Unclassified - unlimited STAR Category 02		
19. Security Classif. (of this report) Unclassified	20. Security Classif. (of this page) Unclassified	21. No. of Pages 24	22. Price* $3.50

COLD-AIR PERFORMANCE OF A TIP TURBINE DESIGNED TO DRIVE A LIFT FAN

I - BASELINE PERFORMANCE

by Jeffrey E. Haas, Milton G. Kofskey, Glen M. Hotz, and Samuel M. Futral, Jr.

Lewis Research Center and
U.S. Army Air Mobility R&D Laboratory

SUMMARY

Full admission baseline performance was obtained for a 0.4 linear scale of the LF460 lift fan turbine over a range of speeds and pressure ratios without leakage air. These cold-air tests covered a range of speeds from 40 to 140 percent of design equivalent speed and a range of scroll inlet total to diffuser exit static pressure ratios from 2.0 to 4.2.

The results of the investigation indicated a total efficiency of 0.815 at design equivalent speed and pressure ratio. This efficiency was based on stator inlet total pressure and rotor exit total pressure. The design efficiency for this turbine was 0.832. The overall static efficiency, based on scroll inlet total pressure and diffuser exit static pressure, was 0.670 as compared to a design value of 0.695.

The equivalent choking mass flow was 3.336 kilograms per second at design equivalent speed and pressure ratio. This flow was 10.1 percent greater than design due to an oversized stator throat area.

The experimental total pressure drops in the scroll, stator, and rotor agreed closely with their respective design values. However, the total pressure drop in the turbine exit diffuser was considerably higher than its design value. This difference was believed due primarily to the absence of fan leakage flow, which was provided for in the design of the full-scale turbine diffuser.

INTRODUCTION

In the past several years a need has been demonstrated for an airplane that has the VTOL capability of a helicopter together with the advantages of the current conventional aircraft with respect to speed, cargo capacity, and fuel economy. V/STOL aircraft of

the fixed-wing type with one or more lift fans are being considered to fill this need for both military and civil applications.

For civil aviation the use of V/STOL aircraft would reduce congestion and noise pollution that exists at many large airports. The ability to take off and land without the use of long runways could permit the diversion of some of the air traffic to smaller airports. The ability to enter and leave the takeoff and landing pattern at higher altitudes would reduce the noise pollution in the surrounding populated areas.

For military service, the fixed-wing V/STOL aircraft would be very useful for a number of missions. It could be used for assault transport, anti-submarine warfare, search and rescue missions, and early warning systems. Several applications are listed in reference 1, which includes a general discussion of airplanes of this type.

Some engine and component arrangements have been considered for providing takeoff and landing lift for this type of aircraft. These are discussed in some detail in references 1 to 3. One arrangement of particular interest is a fan driven by a turbine which is mounted on the rotating shroud of the fan blades. Such a turbine is called a tip-turbine and is supplied by one or more remotely located gas generators. This arrangement has advantages in total weight and in flexibility of locating the various components.

Interest in the performance of a tip-turbine arises because of several of its unique design features. Mounting the rotor blades on the fan shroud results in blades that are short compared to the turbine diameter. Also, large tip clearances and axial clearances must be used to allow for thermal growth and considerable flexure of the fan. These clearances are unusually large compared to the blade size. There is also some concern about losses in the scroll. The scroll is necessarily complex with each half of the scroll serving half of the stator because two gas generators are used for redundancy in case one fails during takeoff or landing.

Reference 4 is the design report of a program sponsored by the NASA-Lewis Research Center to investigate a particular lift fan system. This system has the designation LF460. In order to test the tip turbine from this fan system in an existing Lewis Research Center cold-air component test facility, a 0.4 linear scale of the LF460 tip-turbine was designed and fabricated. A solid disk was used in place of the fan for the test rotor. The rotor clearances were scaled to match the hot running clearances of the full-size turbine. Three series of tests are planned. The first tests are baseline performance tests. The second are partial admission tests with one side of the scroll used at a time to simulate loss of one of the gas generators, and the third are tests to determine the effect of leakage from the fan into the turbine.

This report presents the results of the baseline performance tests which were conducted with air entering the scroll at total conditions of approximately 330 K and 9.10 newtons per square centimeter. The speed range covered was 40 to 140 percent of the design equivalent speed in increments of 10 percent. At each speed increment the total

to static pressure ratio, as based on the scroll inlet total pressure and the diffuser exit static pressure, was varied from approximately 2.0 to 4.2.

In this report, a brief description of the full-scale and scale model turbines is given. Experimental performance maps and curves relating equivalent values of mass flow and torque with pressure ratio, and a breakdown of the total pressure drop in the turbine at the design operating point, are presented. A comparison of test results with design values is made.

SYMBOLS

Δh turbine specific work, J/g

N rotative speed, rpm

p absolute pressure, N/cm^2

$\Delta p'$ total pressure drop, N/cm^2

R_x blade reaction $\left(W_5^2 - W_4^2\right) 2 \Delta h$

T absolute temperature, K

U blade velocity, m/sec

V absolute gas velocity, m/sec

ΔV_u change in absolute tangential velocity, m/sec

W relative gas velocity, m/sec

w mass flow, kg/sec

α absolute gas flow angle measured from axial direction, deg

β relative gas flow angle measured from axial direction, deg

Γ torque, N-m

γ ratio of specific heats

δ ratio of stator inlet total pressure to U.S. standard sea-level pressure, p_3'/p^*

ϵ function of γ used in relating parameters to those using air inlet conditions at U.S. standard sea-level conditions, $(0.740/\gamma)[(\gamma + 1)/2]^{\gamma(\gamma-1)}$

η static efficiency based on pressure ratio, p_1'/p_6

η' total efficiency based on pressure ratio, p_3'/p_5'

θ circumferential position around scroll, deg

θ_{cr} squared ratio of critical velocity at stator inlet temperature to critical velocity at U.S. standard sea-level temperature, $(V_{cr3}/V_{cr}^*)^2$

ω   turbine speed, rad/sec

Subscripts:

cr   condition corresponding to Mach number at unity

eq   equivalent

1   station at scroll inlet (fig. 11)

3   station at stator inlet (fig. 11)

4   station at stator exit (fig. 11)

5   station at rotor exit (fig. 11)

6   station at diffuser exit (fig. 11)

Superscripts:

'   absolute total state

*   U.S. standard sea-level conditions (temperature, 288.15 K; pressure, 10.13 N/cm^2)

TURBINE DESCRIPTION

A brief description of the full-scale turbine will be given first, followed by a description of the scale model turbine. Engine design conditions for the full-scale turbine are presented in table I, along with the design equivalent conditions for the scaled turbine.

Full-Scale Turbine

General description. - The full-scale turbine was designed to drive a lift fan with a nominal 152.4-centimeter tip diameter. Figure 1 presents the basic layout of the fan and drive turbine. This figure is from reference 4. There are two inlets to the scroll which are located adjacent to each other. Each inlet is supplied by a separate gas generator and, in turn, each inlet supplies a different segment of the scroll. The purpose of the dual inlets is for redundancy in case one of the gas generators fails.

Figure 1 shows large axial and radial clearances in the turbine compared to a conventional turbine design. These unusually large clearances were provided because of large thermal growth of the scroll structure and considerable flexure of the fan. A three-chamber scroll was used to provide an even distribution of hot gas to the stator

4

and to form a compact, structurally sound design. The lift-fan system was designed to be compact so that it could be enclosed within the envelope of the wing cross section.

A turbine exit diffuser was used to produce as low a static pressure as possible in the turbine rotor to prevent leakage of hot turbine gas into the fan.

Figure 2 shows the mean-section velocity diagrams for the turbine. As discussed in reference 4 the turbine was a single-stage design with a supersonic stator and a subsonic impulse rotor, based on a zero static pressure drop across the rotor. The turbine rotor had a hub-to-tip radius ratio of about 0.940. A desired feature of the turbine design was to attain a zero radial static pressure gradient in the vicinity of the stator and rotor. This condition was implemented by designing the flow path (fig. 1) with stream-line curvature in the meriodional plane such that the static pressure gradient resulting from this curvature balanced that resulting from the whirl velocity. A design of this type results in nearly constant velocity diagrams from hub to tip and makes possible the use of constant section stator and rotor blading.

Scroll. - The layout of the scroll flowpath is shown in figure 3. As discussed in reference 4 the scroll is divided in half with each half supplied by a separate inlet. Both inlets are located at a common circumferential location. Therefore, the flow in one-half of the scroll is counter to the direction of rotation. At each inlet the scroll is divided into three chambers. Only the large upper chamber continues around the full 180°. The design Mach number for the flow entering the scroll is approximately 0.3. The flow is then turned in the circumferential direction, divided into three chambers on each side, and accelerated to about Mach 0.35. The flow then passes through a cascade of struts, which serve as structural members as well as turning vanes for turning the flow radially inward into a vaneless annulus which turns the flow axially. Each half of the scroll is formed by three intersecting circular ducts of varying radii. The intersections are connected by separator plates to form separate passages. These separator plates have a row of small circular holes down their length to allow static pressure equalization between the chambers.

Stator. - Since the flow in one half of the scroll moves counter to the direction of rotation, three different vane profiles are used to meet the varying flow angles created by the scroll. Figure 4 shows the different vane types and how these vanes are located circumferentially with respect to the scroll. The vane profiles were designed for inlet flow angles of 60°, 0°, and -60°. However, the diverging portion of the passages were geometrically similar for all three types of vanes. The vanes were designed with a convergent-divergent flow passage which resulted in an exit-to-throat area ratio of 1.071. There was a total of 157 vanes.

Rotor. - Figure 5 shows the rotor blade profile. There was a total of 264 rotor blades. The rotor profile is constant from hub to tip. The rotor was designed to operate at impulse conditions to minimize the tip leakage losses. As mentioned previously, large axial and radial clearances were necessary due to fan flexure and shroud growth.

The tip clearance is of the order of 1.3 centimeters, which is approximately 25 percent of the rotor blade height. Thus, impulse blading with shrouded blade tips was chosen to minimize the tip leakage losses.

Diffuser. - The exit diffuser consists of a diverging annular passage with eight struts. The struts serve as structural members to support the fan structure. The exit to inlet area ratio of the diffuser is approximately 1.5.

Scale-Model Turbine

In order to test the LF460 turbine in an existing Lewis Research Center cold air component test facility, it was necessary to design and fabricate a 0.4 linear scale model of this turbine. Figure 6 is a photograph of the scaled turbine installed in the test cell. The photograph was taken from the exhaust end. Visible in this photograph is the inlet and exhaust piping and the scroll assembly.

Figure 7 is a closeup of the scroll and stator assembly in its mounting stand. The trailing edges of some of the stator vanes can be seen in this figure. The scroll chambers of the scaled turbine were rectangular rather than circular as in the full-size turbine. This change was made to simplify the fabrication.

The rotor is shown in figure 8. The rotor disk and blading were machined from a single forging, and a shroud ring was furnace-brazed to the blade tips. As discussed in the INTRODUCTION, the axial and radial tip clearances are scaled from the hot operating condition for the full-scale turbine.

APPARATUS

The apparatus consisted of the turbine, a cradled gearbox, and a cradled dynamometer to absorb the power output of the turbine and to control turbine speed. In addition, there was inlet and exhaust piping with flow controls for setting inlet and exit pressures of the turbine. The arrangement of the apparatus is shown schematically in figure 9. High-pressure dry air was supplied from a central air system. The air passed through a 100-kilowatt heater, a calibrated orifice plate, a remotely controlled turbine-inlet valve, and the two scroll inlets to enter the turbine scroll. Leaving the turbine the air was exhausted through a system of piping and a remotely operated valve into a central low-pressure exhaust system. A 224-kilowatt dynamometer cradled on hydrostatic trunion bearings was used to absorb the turbine power, to control the turbine speed, and to measure the torque. The dynamometer was coupled to the turbine shafting through a

gearbox cradled on hydrostatic bearings. The gearbox provided relative rotative speeds between dynamometer and turbine of 1.0 to 2.0. The stators of the gearbox and dynamometer were coupled together so that the measured torque was the net torque developed by the turbine. Figure 10 shows the dynamometer and gearbox.

INSTRUMENTATION

A torque arm attached to the dynamometer stator and a commercial strain-gage load cell were used to measure the net turbine torque. The load cell output was read on a digital voltmeter. The rotational speed was detected by a magnetic pickup and a shaft-mounted gear. The magnetic pickup output was converted to a direct-current voltage, which was proportional to the frequency, and fed into the digital voltmeter.

State conditions of the flow were determined by measurements taken at the scroll inlet, stator inlet, rotor exit, and diffuser exit. The instrumentation stations are shown in figure 11. The instrumentation at the scroll inlet (station 1) included four static pressure taps in each of the two inlets. A total-temperature rake containing three thermocouples was also located upstream of the two inlets. At the stator inlet (station 3) there were six static pressure taps equally spaced circumferentially along the hub wall. There were also six total pressure probes spaced circumferentially as shown in figure 18(a). Each total pressure probe contained three elements to provide measurements at the mean radius and also near the hub and tip walls. In addition, there was a tube on each side of the mean-section total pressure sensing tube. These two side tubes, which had their sensing ends cut off to form a 90° wedge, were connected to a differential pressure transducer to provide a means for manually alining the probe with the flow. A scale and pointer were attached to each probe to provide an indication of the mean-section flow angle.

At the rotor exit (station 5) there were six single-element Kiel total pressure probes approximately evenly spaced circumferentially. Radially, these probes were spaced so that there were two each near the hub wall, the mean radius, and the tip wall. Use of Kiel type total pressure probes provided accurate total pressure readings over a range of absolute flow angles of about $\pm30^o$. Since the actual absolute flow angle range was greater than $\pm30^o$, it was necessary to readjust the setting angle of the probes during the course of the test program.

At the diffuser exit (station 6) there were eight static pressure taps spaced circumferentially with four each at the inner and outer walls. Two self-alining probes, located 180° apart at the mean radius, were used for measuring total pressure, total temperature, and flow angle.

The values of the pressures at the various stations were measured by unbonded, strain-gage transducers. A 200-channel data acquisition system was used to measure and record the electrical signals from the instrumentation.

PROCEDURE

Data were obtained at nominal scroll inlet total conditions of 330 K and 9.10 newtons per square centimeter. The performance tests covered a range of scroll inlet total to diffuser exit static pressure ratio p_1'/p_6 from approximately 2.0 to 4.2 and a speed range from 40 to 140 percent of design equivalent speed in increments of 10 percent.

Dynamometer-torque calibrations were obtained before and after each daily series of runs. Corrections were applied to the net turbine torque to include the effects of calculated disk windage and measured turbine bearing friction to obtain the turbine aerodynamic torque. At design conditions these corrections amounted to about 1 percent of the measured turbine power.

The turbine was rated on the basis of both total and static efficiency. The total efficiency η' was based on stator inlet total pressure and rotor exit total pressure, while the static efficiency η was based on scroll inlet total pressure and diffuser exit static pressure. At the stator inlet and rotor exit the total pressures were an average of the measured values. At the scroll inlet and diffuser exit the total pressures were calculated from mass flow, total temperature, static pressure, and flow angle. The diffuser exit total temperature was calculated from the measured scroll inlet total temperature and the turbine work. When calculating the scroll inlet total pressure, the flow angle was assumed to be zero.

RESULTS AND DISCUSSION

Performance results are presented for a 0.4 linear scale of the LF460 lift fan turbine. Performance tests were conducted at nominal scroll inlet total conditions of 330 K and 9.10 newtons per square centimeter. The range of speed covered was 40 to 140 percent of design equivalent speed, and the range of scroll inlet total to diffuser exit static pressure ratio p_1'/p_6 was approximately 2.0 to 4.2. Experimental results include performance in terms of equivalent mass flow, equivalent torque, equivalent specific work, and efficiency. Also included is a breakdown of the total pressure drop through the turbine.

Mass Flow

Figure 12 shows the variation of equivalent mass flow $\epsilon w \sqrt{\theta}/\delta$ with total pressure ratio p_3'/p_5'. The figure indicates that the stator was choked over the whole range of speed and pressure ratio investigated. The choking mass flow was 3.336 kilograms per second, which was approximately 10.1 percent greater than the design mass flow of 3.03 kilograms per second. The equivalent mass flow was calculated based on the stator inlet total pressure. Thus, the higher than design mass flow indicates that the stator throat area was oversized.

Equivalent Torque

Figure 13 shows the variation of equivalent torque $\epsilon \Gamma/\delta$ with total pressure ratio p_3'/p_5' for lines of constant speed. An equivalent torque value of 392 newton-meters was obtained at design equivalent speed and pressure ratio. This is about 8.0 percent larger than design. This larger torque value occurred partly because the mass flow was 10.1 percent greater than design. Since the torque was 8.0 percent greater than design and the mass flow 10.1 percent greater than design, it is apparent that the turbine efficiency must be approximately 2.0 percent less than design. The torque curves show a continuous increase with pressure ratio, indicating that limiting loading was not achieved.

Turbine Efficiency

A performance map for this turbine is shown in figure 14. This performance map is based on the total pressure ratio from the stator inlet to the rotor exit. The map shows equivalent specific work $\Delta h/\theta_{cr}$ as a function of mass-flow-speed parameter $\epsilon w \omega/\delta$ for the various equivalent speeds investigated. Lines of constant pressure ratio p_3'/p_5' and total efficiency η' are superimposed. A total efficiency of 0.815 was obtained at design equivalent speed and pressure ratio. This was 0.017 lower than the design efficiency of 0.832. A maximum total efficiency of 0.850 was attained between 110 and 120 percent equivalent speeds at a pressure ratio of 3.0.

Figure 15 shows turbine velocity diagrams as calculated from experimental data at design equivalent speed and near design equivalent pressure ratio. These velocity diagrams were calculated based on mass-averaged conditions across the turbine. The rotor exit diagram was constructed using the average measured rotor exit total pressure, the design rotor exit relative gas angle, and an iterative method to calculate the rotor exit absolute flow angle and static pressure. The stator exit diagram was constructed from the rotor exit conditions and the measured equivalent specific work. In addition, a measurement of the static pressure on the upstream side of the rotor disk was assumed

9

to represent the stator exit static pressure. Using this assumption, the total pressure and absolute flow angle at the stator exit could be calculated using an iterative method.

Values of rotor reaction R_x and rotor incidence angle were calculated using the velocity diagrams in figure 15. The rotor reaction was -0.031 compared to a design value of -0.099 as calculated from figure 2. The rotor incidence angle was 1.9° compared to a design value of 4.5°. The small deviation in incidence angle from its design value would not be expected to affect the turbine efficiency. However, the slightly less negative reaction caused a slight decrease in static pressure through the rotor.

The iterative methods used to calculate the stator and rotor exit absolute flow angles produced values of 65.4° and 6.8°, respectively. Both angles were close to their respective design valves.

In addition, values of stator and rotor efficiency were calculated from the experimental velocity diagrams. The stator efficiency was 0.967 compared to a design value of 0.963. The stator efficiency is defined as a ratio of the actual stator exit kinetic energy to the ideal stator exit kinetic energy, which is based on the stator inlet total to stator exit static pressure ratio. The rotor efficiency was 0.847 compared to a design value of 0.872. The rotor efficiency is defined as the ratio of the actual turbine work to the ideal turbine work, which is based on the rotor inlet absolute total to rotor exit absolute total pressure ratio. The lower than design rotor efficiency was believed due to an excessive tip clearance penalty. Reference 5 indicates that a decrease in turbine work of 7.8 percent would be predicted for a shrouded, impulse rotor with a tip clearance that is 25 percent of the rotor blade height. For this reference turbine rotor, the designation impulse implied a constant relative velocity through the rotor. Therefore, a slight decrease in static pressure existed through the rotor, similar to the subject turbine. For the LF460 test turbine this decrease in turbine work would correspond to about 6.5 percentage points in turbine efficiency.

Figure 16 shows a performance map for the test turbine which is based on scroll inlet total to diffuser exit static conditions. At equivalent design conditions of speed and pressure ratio, the static efficiency was 0.670 compared to a design value of 0.695. This decrease in efficiency from the design value was believed due, in part, to a reduced static pressure rise in the diffuser due to a higher than design diffuser total pressure drop.

Total Pressure Drop

Of importance in this discussion of the turbine performance is a comparison of the measured and the design total pressure drops through the turbine. Table II lists both the static and total pressures at the various turbine measuring stations at design equivalent speed and near design equivalent pressure ratio. As mentioned in the section PROCE-

10

DURE, the values of total pressure at the scroll inlet and the diffuser exit were calculated from the static pressure, total temperature, mass flow, and flow angle. When the boundary layer is thin, the calculated total pressure will be very close to the true total pressure. In the case where the flow is separated and there is considerable jet flow the calculated total pressure will be low and will correspond to a mixed-out value. The values of total pressure at the stator inlet and rotor exit are an average of the measured values. The stator exit total pressure was calculated from an iterative method.

Table III shows a comparison of the experimental and design total pressure drops through the turbine. These total pressure drops are expressed as a ratio of total pressure drop divided by the scroll inlet total pressure $\Delta p'/p_1'$. Figure 17 shows these total pressure drops plotted on a bar graph. As seen from table III and figure 17, the total pressure drops in the scroll, the stator, and the rotor were very close to their respective design values.

Figure 18(a) shows the circumferential variation of stator inlet total pressure. Total pressure measurements were made at the mean position and near the hub and tip walls at six different circumferential positions. There was a maximum 18 percent variation in total pressure circumferentially. The variation in total pressure from positions D to F was as expected. However, the high loss at position B was not as expected. The reason for the deviation from the expected variation of positions A to C was not determined.

Figure 18(b) shows the circumferential variation of stator inlet mean flow angle. This flow angle was obtained at each position by manually alining the probe with the flow and using the pointer and scale attached to the probe to indicate the flow angle. The trend in the flow angle is toward less turning from 45° to 135° and from 225° to 315°. From positions A to C the average flow angle was 63°. From positions D to F the average flow angle was 54.5°.

As mentioned earlier in this section, the total pressure drops across the scroll, stator, and rotor were close to their respective design values; however, table III and figure 17 show that the diffuser total pressure drop was considerably higher than design. However, as discussed in reference 4, the effect of leakage flow from the fan into the diffuser inlet was taken into consideration in the diffuser design. Since this leakage flow was not present in the test turbine, the performance of the diffuser and, to some degree, the overall static efficiency are not representative of the performance of the full-scale turbine.

SUMMARY OF RESULTS

Full admission baseline performance was obtained for a 0.4 linear scale of the LF460 lift fan turbine over a range of speeds and pressure ratio. These cold-air tests were baseline performance tests without leakage air. The results of this investigation may be summarized as follows:

1. A total efficiency of 0.815 was obtained at design equivalent speed and pressure ratio. This efficiency was based on the total pressure ratio from the stator inlet to the rotor exit. This efficiency was 0.017 less than the design efficiency of 0.832. A maximum total efficiency of 0.850 was obtained between 110 and 120 percent equivalent speeds at a pressure ratio of 3.0.

2. A mass flow of 3.336 kilograms per second was obtained at design equivalent speed and pressure ratio. This mass flow was constant over the range of speeds and pressure ratios investigated and was approximately 10.1 percent greater than the design mass flow due to an oversized stator throat area.

3. An overall static efficiency of 0.670 was obtained at design equivalent speed and design equivalent scroll inlet total to diffuser exit static pressure ratio. This efficiency was 0.025 less than the design value of 0.695. This difference in efficiency was attributed in part to a higher than design diffuser total pressure drop.

4. Total pressure drops in the scroll, stator, and rotor closely agreed with their respective design values. However, the total pressure drop in the diffuser was considerably higher than its design value. This difference in total pressure drop was believed due primarily to the absence of fan leakage flow, which was provided for in the design of the full-scale turbine diffuser.

Lewis Research Center,
    National Aeronautics and Space Administration,
        and
U.S. Army Air Mobility R&D Laboratory,
    Cleveland, Ohio,
        505-05.

REFERENCES

1. Novak, Lloyd R.: The Lift/Cruise Fan Multimission V/STOL Aircraft. AIAA Paper 75-277, Feb. 1975.

2. Dugan, James F., Jr.; et al.: Preliminary Study of an Air Generator-Remote Life Fan System for VTOL Transports. NASA TM X-57916, 1971.

3. Gertsma, L. W.; and Zigan, S.: Propulsion System for Research VTOL Transports. ASME Paper 73-GT-24, Apr. 1973.

4. LF460 Detail Design. (General Electric Co.; NAS2-6056) NASA CR-120787, 1971.

5. Kofskey, Milton G.: Experimental Investigation of Three Tip-Clearance Configurations over a Range of Tip Clearance Using a Single-Stage Turbine of High Hub-to-Tip Radius Ratio. NASA TM X-472, 1961.

TABLE I. - TURBINE DESIGN CONDITIONS

Parameter	Full-scale engine	Scale model equivalent
Stator inlet temperature, T_3', K	1144	288.2
Stator inlet pressure, p_3', N/cm^2	37.7	10.13
Mass flow rate, w, kg/sec	34.6	3.03
Rotative speed, N, rpm	4300	5395
Specific work, Δh, J/g	268.4	67.6
Torque, Γ, N-m	20623	363
Power, kW	9290	205
Pressure ratio, p_3'/p_5'	3.05	3.16
Pressure ratio, p_1'/p_6	3.92	4.10
Total efficiency, η_{3-5}	0.832	0.832
Work factor, $\Delta V_u/U$	1.982	1.982

TABLE II. - TOTAL AND STATIC PRESSURE DIS-

TRIBUTION FOR SCALE MODEL TURBINE AT

DESIGN EQUIVALENT SPEED AND NEAR

DESIGN EQUIVALENT PRESSURE RATIO

Station (a)	Static pressure, p, N/cm^2	Total pressure, p', N/cm^2
1 (scroll inlet)	8.55	9.09
3 (stator inlet)	8.08	8.51
4 (stator exit)	2.23	8.09
5 (rotor exit)	2.13	2.75
6 (diffuser exit)	2.00	2.30

[a]See fig. 11 for station location.

TABLE III. - TOTAL PRESSURE DROP FOR SCALE MODEL

TURBINE AND FULL-SCALE TURBINE

Station (a)	Scale model turbine		Design values for full-scale turbine, $\Delta p'/p_1'$, percent
	Total pressure drop, [b] $\Delta p'$, N/cm^2	Pressure ratio, [b] $\Delta p'/p_1'$, percent	
1 to 3 (scroll inlet to stator inlet)	0.58	6.4	5.3
3 to 4 (stator inlet to stator exit)	.42	4.6	5.6
4 to 5 (stator exit to rotor exit)	5.34	58.7	58.1
5 to 6 (rotor exit to diffuser exit)	.45	5.0	.4

[a] See fig. 11 for station location.

[b] Data experimentally obtained at design equivalent speed and near-design total pressure ratio.
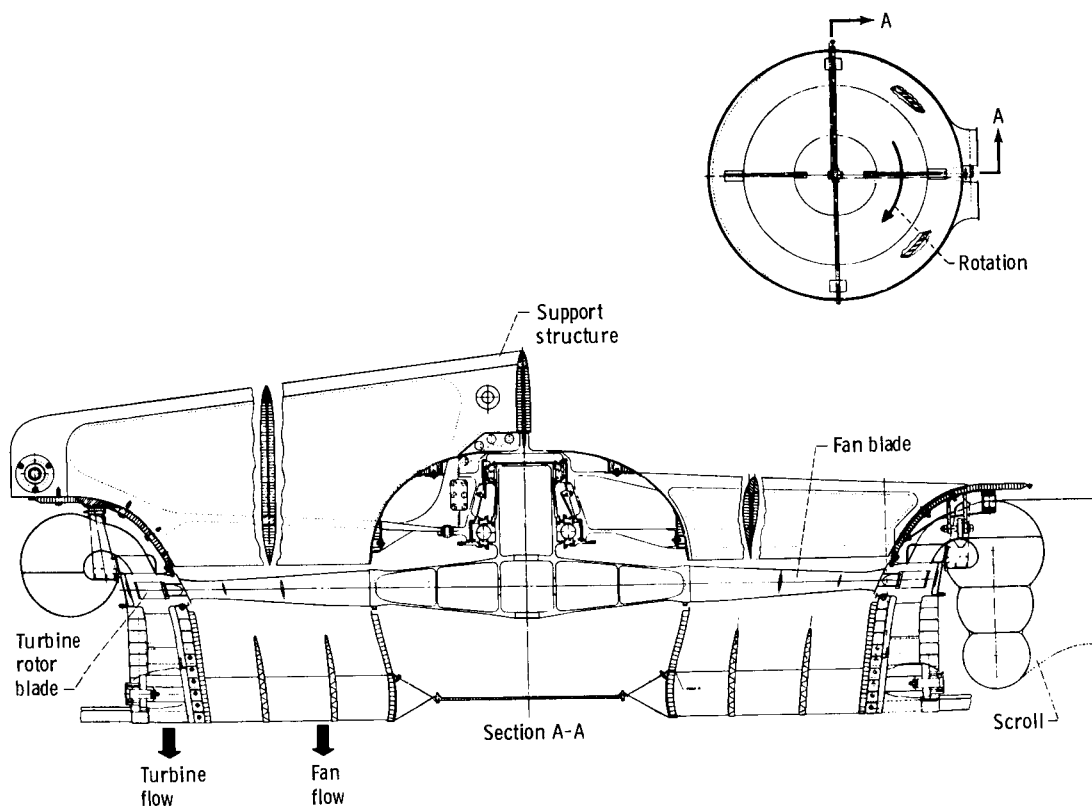
Figure 1. - Lift-fan assembly.

Station

3

$\frac{V}{V_{cr}} = 1.370$

$\frac{W}{W_{cr}} = 0.938$

α

β

4

$\frac{U}{V_{cr}} = 0.597$

α

β

$\frac{W}{W_{cr}} = 0.842$

$\frac{V}{V_{cr}} = 0.669$

5

$\frac{U}{V_{cr}} = 0.669$

	α	β
Station 4	66.3°	50.0°
Station 5	7.3°	-43.0°
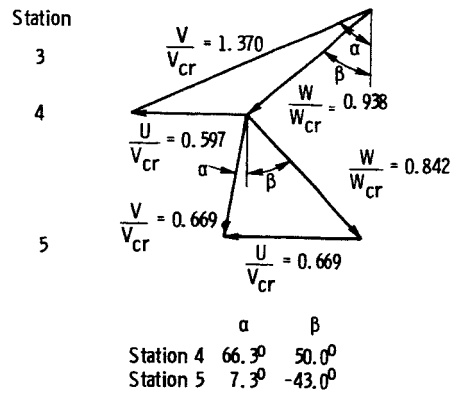
Figure 2. – Design velocity diagrams for LF460 turbine at mean section.
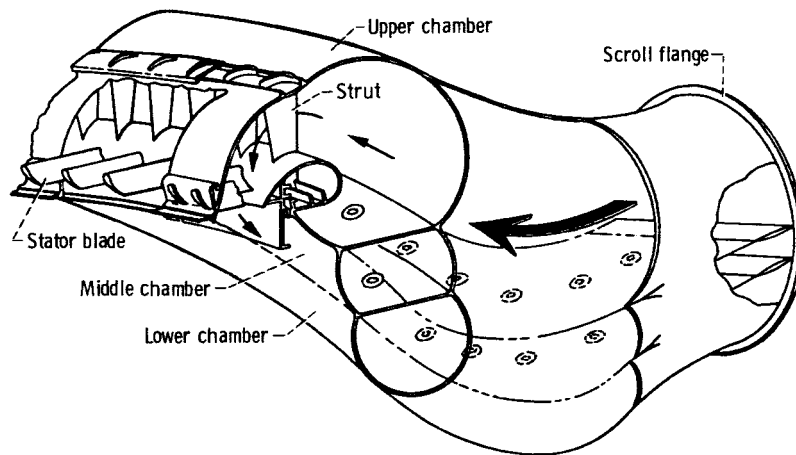
Figure 3. – Scroll flowpath for full-scale turbine.

15

(a) Stator vane profiles.	(b) Location of stator vane types viewed from exhaust end.
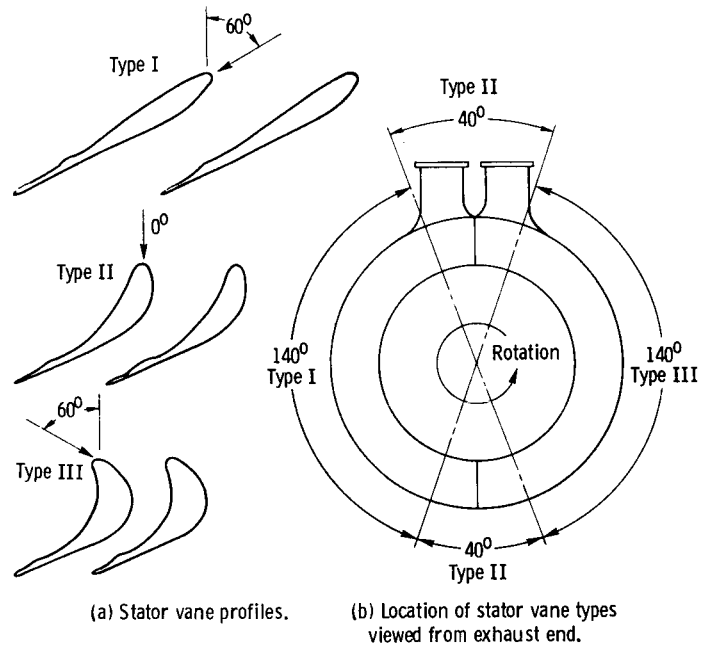
Figure 4. - Sketch showing stator vane profiles and locations.
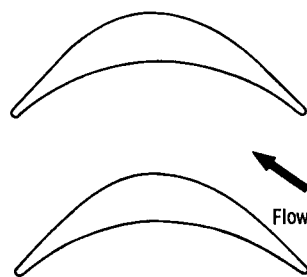
Figure 5. - Rotor blade profile.
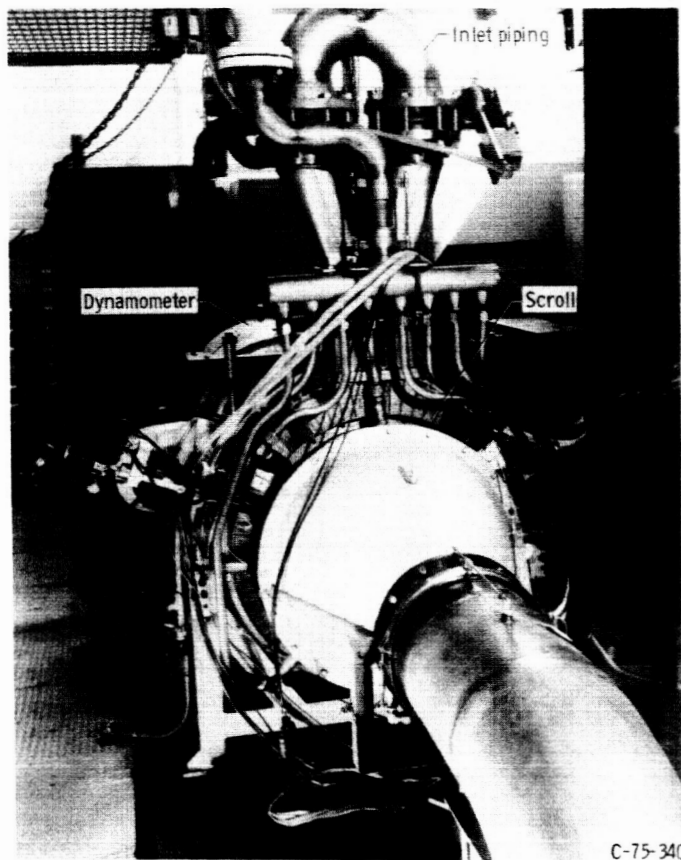
Figure 6. - Turbine test installation.
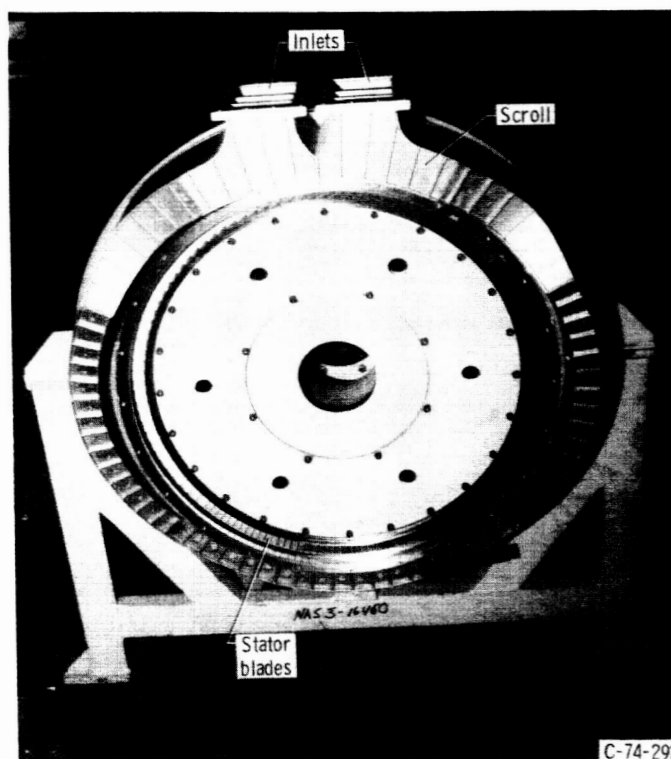
Figure 7. - Test scroll and stator.

Figure 8. - Test rotor.
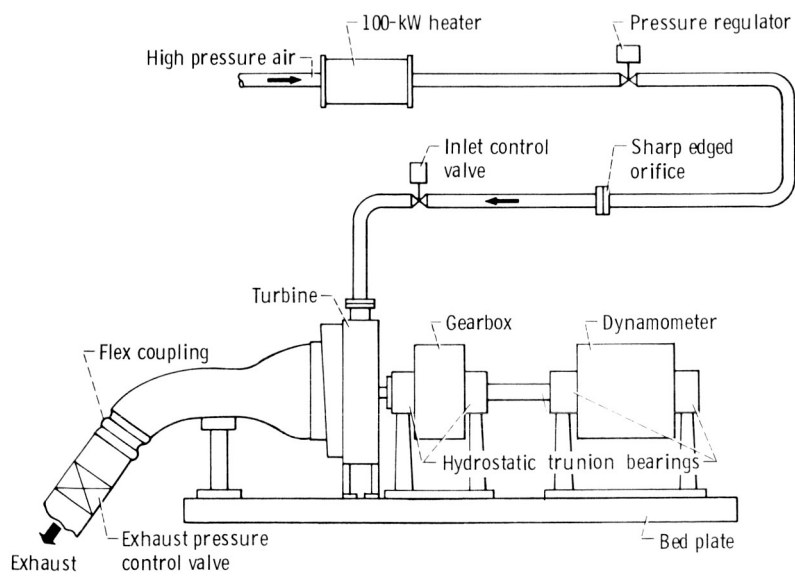
Figure 9. - Test installation diagram.
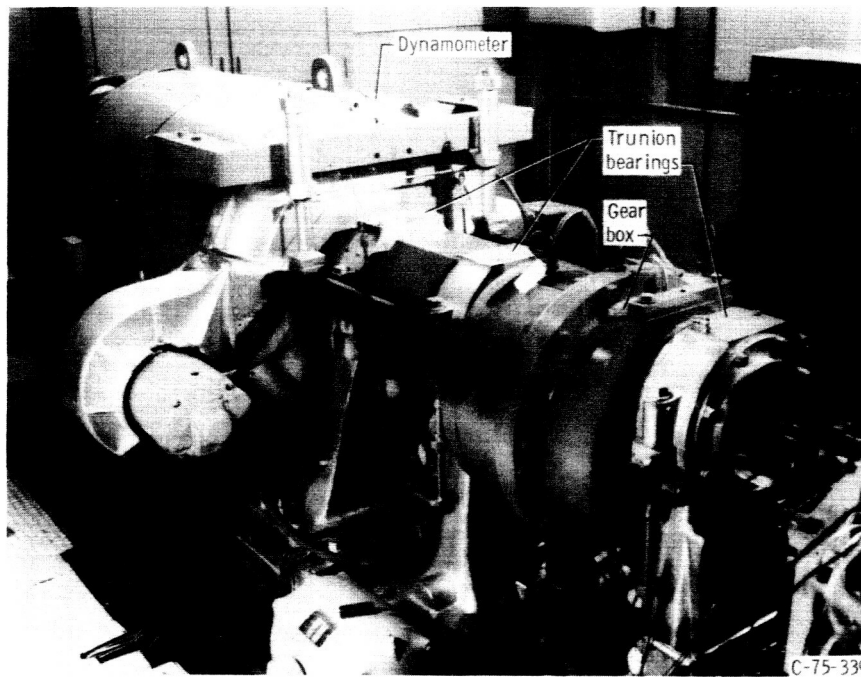
Figure 10. - Dynamometer and gear box.
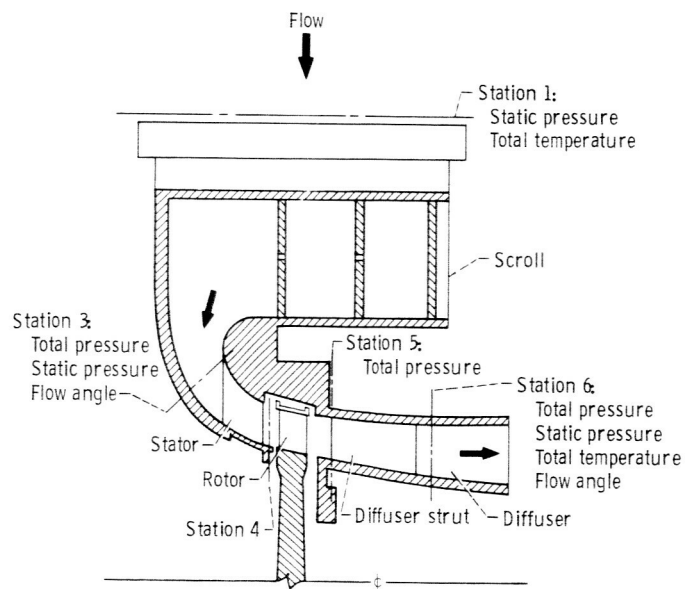
Figure 11. - Schematic of turbine.
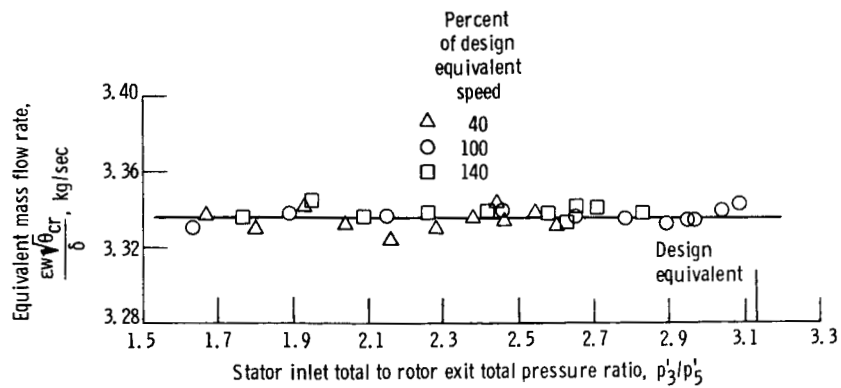
Figure 12. - Variation of mass flow rate with pressure ratio.
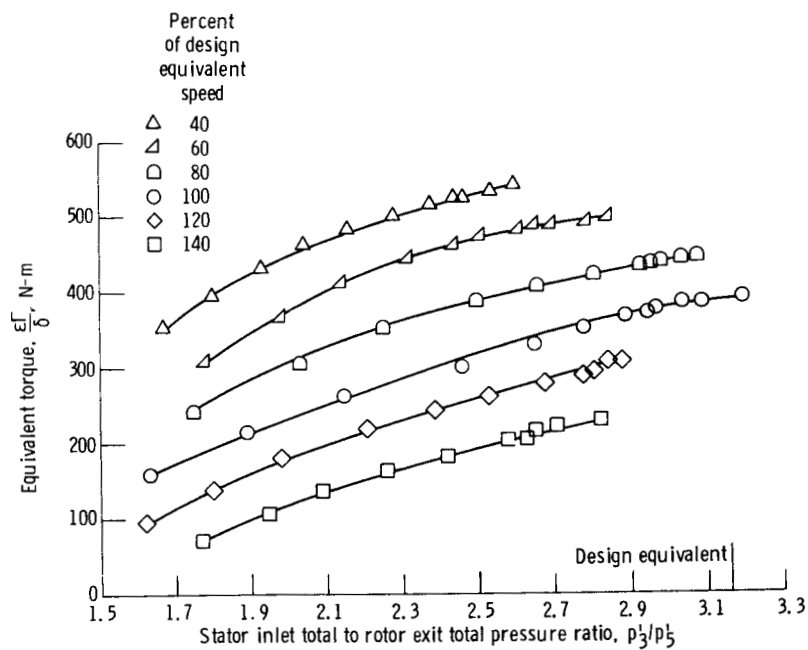
Figure 13. - Variation of torque with pressure ratio.

20
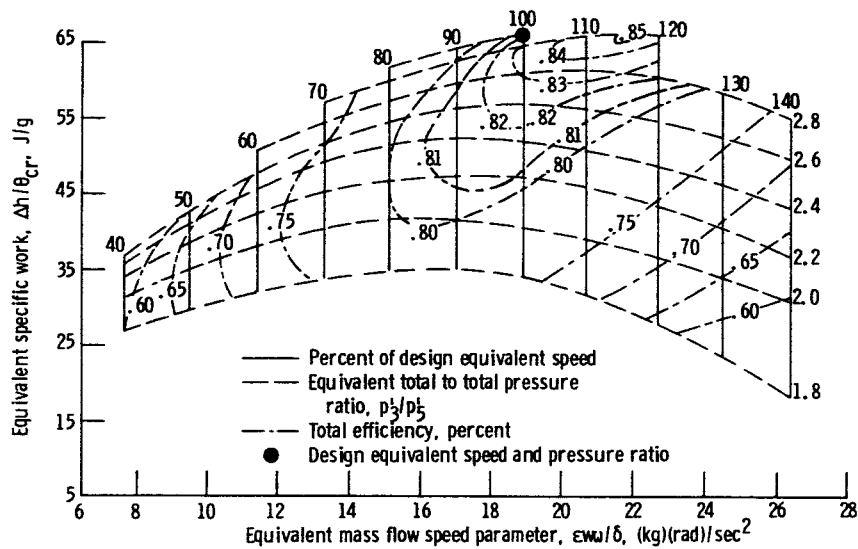
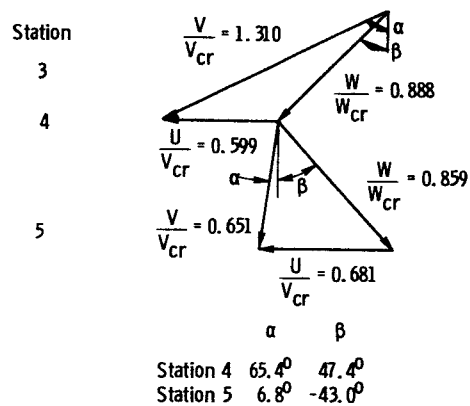Figure 14. – Scale-model turbine performance based on stator inlet total to rotor exit total pressure ratio.

	α	β
Station 4	65.4⁰	47.4⁰
Station 5	6.8⁰	-43.0⁰

Figure 15. – Velocity diagrams for scale-model turbine as calculated from experimental results of design speed and near design pressure ratio.
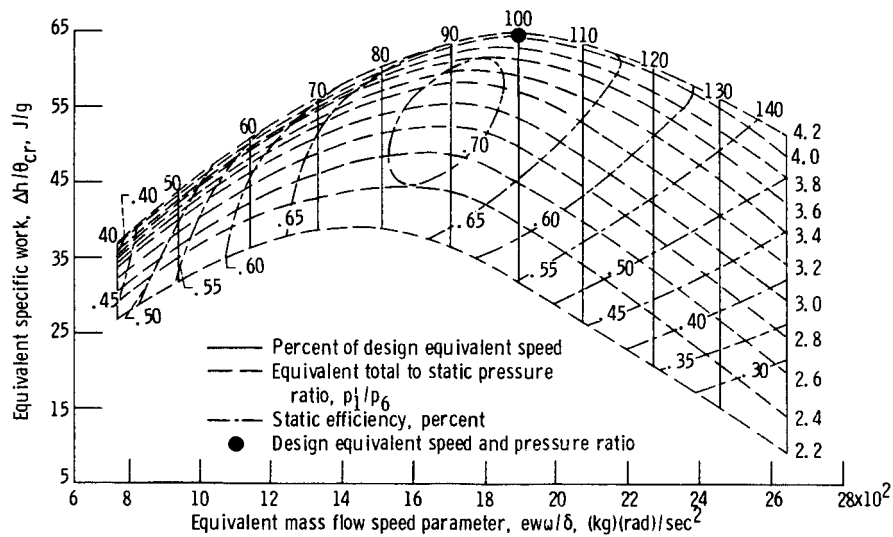
Figure 16. – Scale-model turbine performance based on scroll inlet total to diffuser exit static pressure ratio.
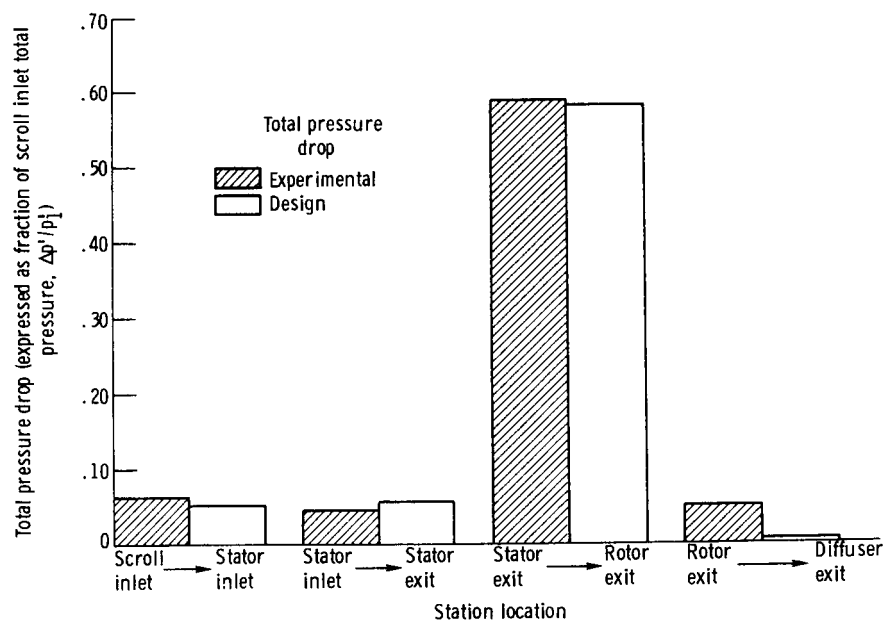

Figure 17. – Comparison of experimental and design total pressure drops through scale-model turbine.

(a) Stator inlet total pressure.
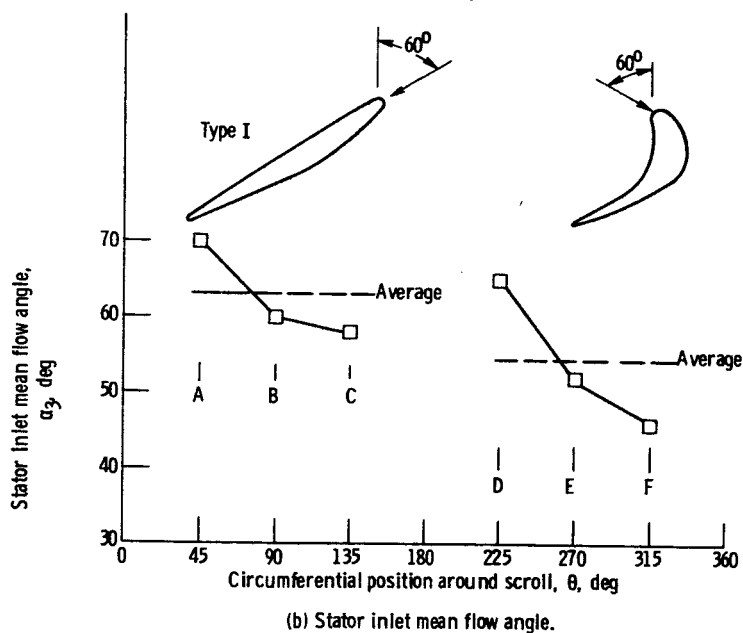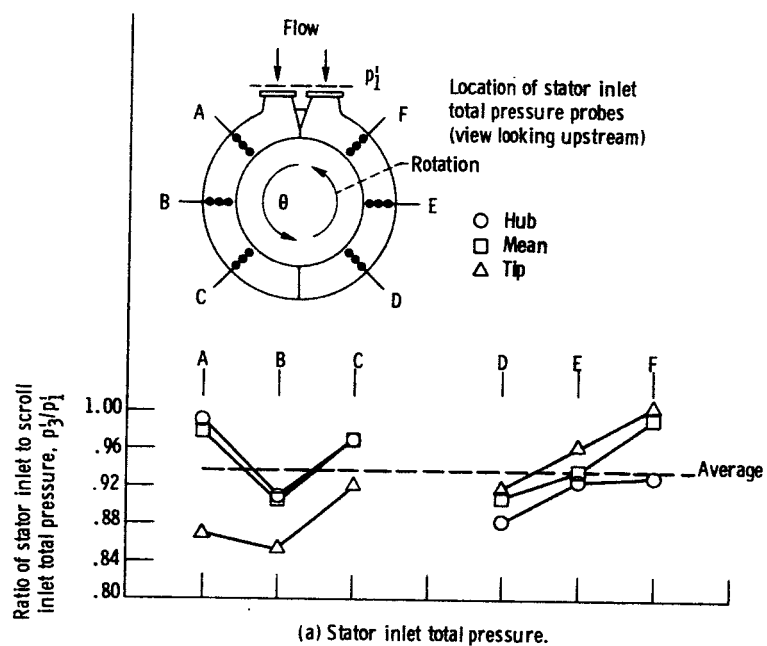
(b) Stator inlet mean flow angle.

Figure 18. - Variation of stator inlet total pressure and stator inlet mean flow angle with circumferential position for scale-model turbine.